

# INFLUENCE OF DIFFERENT SURFACE MATERIALS ON THE FOULING PROCESS IN A MICROSTRUCTURED HEAT EXCHANGER UNDER LAMINAR REGIME

W. Benzinger<sup>1</sup>, J.J. Brandner, U. Schygulla and K. Schubert

Forschungszentrum Karlsruhe  
Institute for Micro Process Engineering  
P.O.Box 3640,  
76021 Karlsruhe, Germany  
e-mail:<sup>1</sup> [benzinger@imvt.fzk.de](mailto:benzinger@imvt.fzk.de)

## ABSTRACT

Microstructure devices are well known for their excellent performance with regard to heat and mass transfer. Microstructured heat exchangers show significant advantages in comparison with conventional heat exchangers. The unique properties of a microreaction system show high overall heat transfer coefficients for example. Small characteristic dimensions are in the order of a few hundred  $\mu\text{m}$  (Schubert et al., 1998, 2001; Wörz et al., 1998). Due to the small dimensions, an increased pressure drop is combined with excellent heat transfer properties. But the small channels are prone to fouling processes. The accumulation of crystalline deposits is a severe problem. An additional wall layer causes a decrease of the overall heat transfer coefficient. Therefore the attention has been directed to the reduction of possible fouling processes within the channels.

The fouling can be subdivided in two parts: First into the induction period and second into the so-called fouling period itself (Lund et al., 1981; Förster et al., 1999a, 1999b, and 2000).

For the investigations a special electrically heated micro heat exchanger with changeable foils of different surface materials (stainless steel, FEP, DLC) was developed. The foil temperature is electronically controlled to a constant level of  $100^\circ\text{C}$ .

A solution of calciumnitrate/sodiumhydrogencarbonate is pumped under laminar flow conditions through the channels of the microstructured part. The high temperature causes the precipitation of solid calciumcarbonate on the surface.

The results for all materials, the uncoated stainless steel and the DLC and FEP coated heat transfer surfaces, show typical fouling behaviour with an induction period, followed by an asymptotic built-up of the deposited calcium carbonate. The fouling plot of DLC and FEP coated heat transfer surfaces contradict the hypothesis that the use of such materials leads to much longer induction periods. There is no influence of the surface material found on the induction period and the gradient of the fouling period in the laminar flow regime.

## INTRODUCTION

Depending on the application micro heat exchangers are developed and fabricated in various sizes for cross flow and counter flow operation. They are characterized by thousands of microchannels per flow passage. The huge number of channels results in specific heat transfer surfaces of up to  $15000\text{ m}^2/\text{m}^3$ . With water as test fluid overall heat transfer coefficients up to  $25000\text{ W}/\text{m}^2\text{K}$  and thermal power up to  $20\text{ kW}$  have been obtained. They are achieved with microstructured heat exchangers in cross flow design with a transfer volume of one cubic-centimeter. These values exceed those of conventional heat exchangers by far. The channels show dimensions in the order of a few hundred  $\mu\text{m}$  which are responsible for the outstanding heat and mass transfer properties. Therefore the attention has been directed to the reduction of possible fouling processes within the microchannels.

Fouling processes cause an additional layer between the heat transfer surface and the fluid. The insulation effect of the deposit contributes to the overall heat transfer coefficient declining the performance of the microstructured heat exchanger dramatically. The reduced efficiency of a heat exchanger can be described by

$$R_f = \frac{1}{k_f} - \frac{1}{k_0} \quad [\text{W}/\text{m}^2\text{K}] \quad (1)$$

which describes the increase of the fouling resistance in the so-called fouling period (Förster et al., 1999, 1999, 2000; Tautz et al., 1971).

$k_0$  is the overall heat transfer coefficient for the clean heat transfer surface and  $k_f$  is the overall heat transfer coefficient for the fouled heat transfer surface, respectively. In the fouling period a continuous growth of an additional wall layer is observed and, hence, a continuous increase of the fouling resistance. In the preceding induction period nuclei at the heat transfer surface are formed and the growth of the fouling layer starts (Lund et al., 1981; Förster et al., 1999, 1999, and 2000).

Both periods consist of two processes, a deposition process and a removal process, respectively. In the deposition process ions diffuse from the bulk to the surface and in a chemical reaction the substances which cause the fouling layer are formed on the surface. The removal of the unwanted deposits is mainly influenced by shear stress forces due to the fluid flow and the adhesive strength of the substances to the surface.

Modification of the interfacial characteristics at the interface heat transfer surface/deposit by the choice of different surface materials decreasing the adhesive strength between deposit and heat transfer surface should result in an increase of the induction period.

The fouling period consists of a deposition process and a removal process. The removal rate can be increased by use of different materials with special surface characteristics. Lower adhesive strength of the surface materials results in less adhesion of the crystalline deposit to the surface. The deposit can be removed much more easily.

Different surface materials with known energetic properties should be compared with each other. For the experiments two different surface coatings have been used: DLC (diamond like carbon) and a FEP coating (fluorinated ethylene propylene). Both are compared with stainless steel (1.4435).

## EXPERIMENTAL

To evaluate the dependence of different surface materials at the interface deposit/heat exchanger to the fouling several surface materials have been used.

For the investigations an electrically heated micro heat exchanger was developed. The device consists of a microstructured part (polycarbonate) with 17 channels. For a comfortable replacement of different surface materials the heat transfer surface is made of a foil, which can easily be replaced. Microstructured part and metallic foil are connected to the top of an electrically heatable aluminium block. The surface temperature is controlled electronically to a constant level of 100°C.

The experimental equipment consists essentially of three parts:

- the oval shaped microstructured device (45 mm length x 25 mm width x 5 mm height) made of polycarbonate material with 17 channels (25 mm length x 800 µm width x 100 µm height), which is fixed on the foil. The microstructured device is sealed with a polymer ring to the foil; both are screwed tightly with a cover plate to the aluminium block. Both cover plate and microstructured device are transparent
- the foil with a thickness of 0.2 mm. The surface materials used for the investigations are stainless

steel, a FEP coated stainless steel foil and a DLC coated stainless steel foil.

- the aluminium block (80 mm length x 50 mm width x 30 mm height) with 2 holes at the lower end to insert heater cartridges (P=200W); at the upper end a thermocouple to control the surface temperature is placed centrally under the foil and the microstructured device.

Photos of the test arrangement are shown in figure 1; details of the foils used can be seen in figure 2. The used surface materials differ by their interfacial characteristics. Properties like roughness, surface topography are not determined.

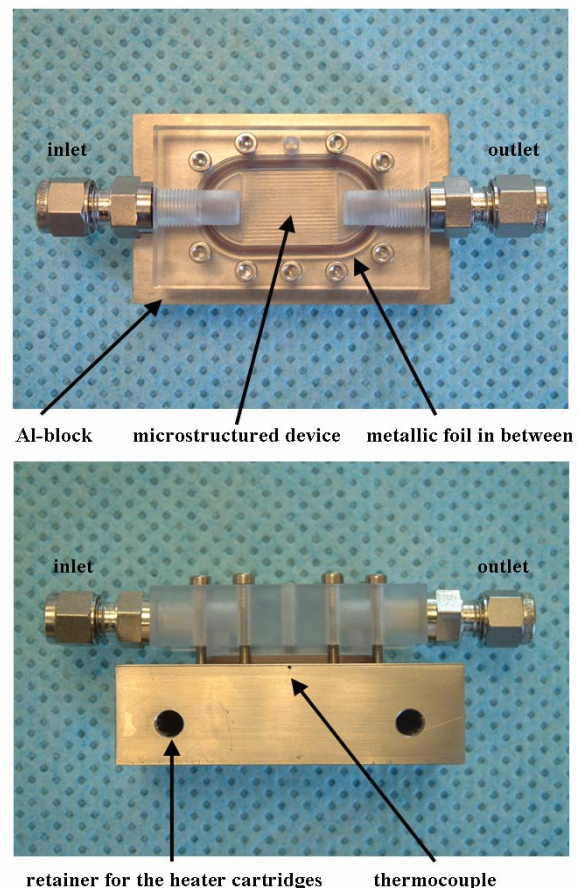


Figure 1: Photos of the test arrangement. Upper picture shows top view of the test arrangement; lower picture shows side view of test arrangement.

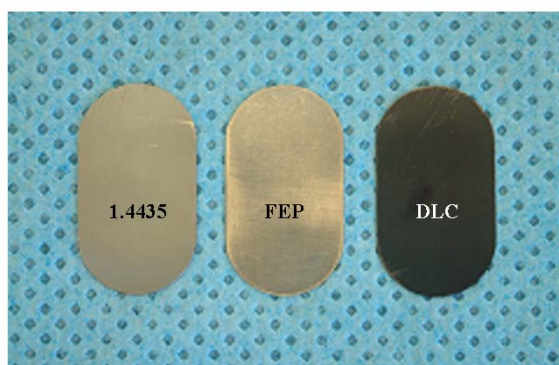


Figure 2: From left to right: metallic foil (stainless steel), FEP and DLC coated metallic foil.

The microstructured device made of a transparent plastic material is shown in figure 3.

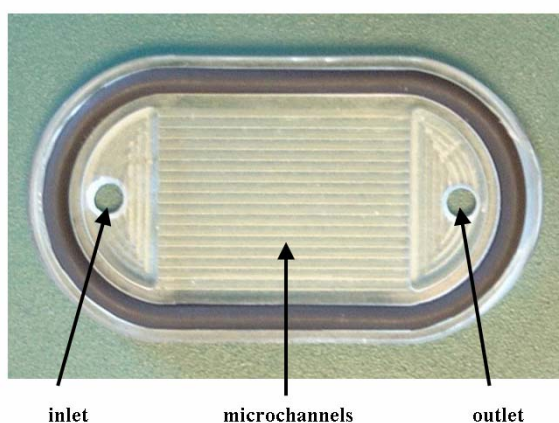


Figure 3: Photo of microstructured device made of a transparent plastic material.

Table 1: Properties of the microstructured device and the metallic foil.

| material                              | polycarbonate            |
|---------------------------------------|--------------------------|
| number of channels,-                  | 17                       |
| length of channels $l$ , mm           | 25                       |
| height of channels, $\mu\text{m}$     | 100                      |
| width of channels $w$ , $\mu\text{m}$ | 800                      |
| width of bars, $\mu\text{m}$          | 200                      |
| thickness of the foil $d$ , mm        | 0,2                      |
| foil material                         | stainless steel (1.4435) |
| area $A$ , $\text{mm}^2$              | 340                      |

The properties of the microstructured device and the metallic foil can be seen in table 1.

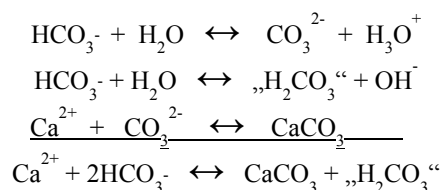
The microstructured device is connected to the metallic foil, which itself is placed on the electrically heatable aluminium block. The temperature of the aluminium block ( $\vartheta$ ) is set to  $100^\circ\text{C}$ . The surface temperature and the “wall” temperature of the foil, respectively, are kept at a constant level (Tautz et al., 1971). The high thermal conductivity of the aluminium ( $\lambda = 200 \text{ W m}^{-1} \text{ K}^{-1}$ ) effects a balanced temperature distribution over the surface, where the metallic foil is placed. Because the microstructured device is made of a polymer it has a low thermal conductivity, which leads to a heat transfer through the metallic foil only. The heat transfer depends on one dimension only (thermal boundary condition of the first kind (Shah et al., 1978)). The aqueous solution is pumped through the microchannels over the hot surface of the metallic foil with a constant temperature level ( $\vartheta_{\text{wall}} = \text{const.}$ ). The temperature of the aqueous solution is measured by two thermocouples in the inlet and outlet in order to determine the fouling resistance. The pressure is measured before and after the microstructured device. The mass flow is determined by a flow meter (coriolis type). All experiments are done under conditions given in Table 2. The process parameters were kept constant.

Table 2: Experimental conditions (laminar regime).

|  |      |
|--|------|
| $T_{\text{inlet}}$ , $^\circ\text{C}$                            | 25   |
| $T_{\text{outlet}}$ , $^\circ\text{C}$ ( $t=0$ )                 | 87   |
| wall temperature $\vartheta_{\text{wall}}$ ,<br>$^\circ\text{C}$ | 99   |
| total massflow, kg/h   | 1,5  |
| massfl. per channel, kg/h  | 0,09 |
| flow velocity, m/s   | 0,3  |
| $Re$ , -   | 110  |
| $\Delta p_{\text{measured}, t=0}$ , mbar                         | 50   |

The fouling experiments are carried out in the test arrangement with the microstructured device integrated in a test rig. The test solution is prepared in deionised water using calcium nitrate/sodium hydrogen carbonate. Both substances are of analytical grade. They are mixed in a ratio 4,48 mmol/l  $\text{Ca}(\text{NO}_3)_2$  to 8,96 mmol/l  $\text{NaHCO}_3$ . The concentration of  $\text{Ca}^{2+}$  is equivalent to a water hardness of  $^\circ\text{d} = 25$ . The concentration is kept constant while the experiments. The test solution is stored in an 80 l vessel and kept to a constant temperature of  $25^\circ\text{C}$ . The pH-value is

kept to pH 7. The heating of the aqueous solution of  $\text{Ca}(\text{NO}_3)_2/\text{NaHCO}_3$  causes the formation of calcium-carbonate. At elevated temperature the formation and precipitation of calcium carbonate on the hot metallic foil of the microstructured heater occurs. This can be described by the following chemical reactions.



The aqueous solution of  $\text{Ca}(\text{NO}_3)_2/\text{NaHCO}_3$  is pumped from the vessel through a filter (SWAGELOK, Type TF) to avoid sedimentation of particles to the microchannels of the microstructured device at a total mass flow of 1.5 kg/h. The massflow per channel equals 0,09 kg/h. This corresponds to a flow velocity of 0,3 m/s. The Reynolds-number is calculated to 110. The aqueous solution is heated up to a temperature level higher than the solubility temperature of  $\text{CaCO}_3$  ( $\text{CaCO}_3$  shows an inverse solubility). The heat causes a precipitation of white particles which stick to the wall. The additional layer consequently reduces the heat transfer properties.

Also first orientating tests in the turbulent flow regime have been performed in a micro heat exchanger. The equipment used is almost the same as in the tests above. To realize turbulent flow conditions the microstructured device has to be changed to a 2-channel system (Figure 4).

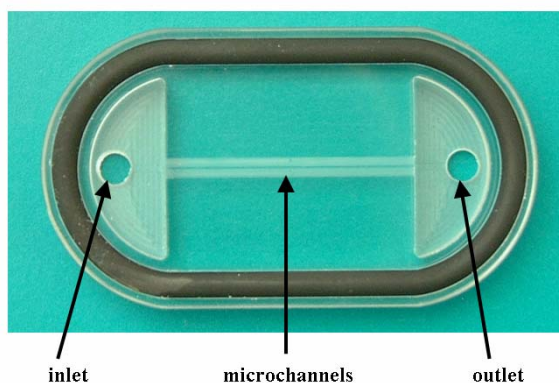


Figure 4: Photo of microstructured device made of a transparent plastic material with 2 channels only.

Table 3: Experimental conditions (turbulent regime).

|  |      |
|--|------|
| $T_{\text{inlet}}, ^\circ\text{C}$                         | 22   |
| $T_{\text{outlet}, t=0}, ^\circ\text{C}$                   | 34   |
| wall temperature $\vartheta_{\text{wall}}, ^\circ\text{C}$ | 99   |
| total massflow, kg/h                                       | 7,0  |
| massfl. per channel, kg/h                                  | 3,5  |
| flow velocity, m/s   | 12,2 |
| Re, -  | 2540 |
| $\Delta p_{\text{measured}, t=0}, \text{bar}$              | 4,98 |

The experimental conditions differ only in the massflow that has been chosen (table 3). This massflow results in a Reynolds' number calculated to 2540.

The aqueous solution gets heated to 34°C only. The temperature is too low for the precipitation of calcium carbonate, which leads to no fouling resistance in dependence on time.

With a simple estimation the surface temperature of the metallic foil made of stainless steel can be evaluated:

$$T_{\text{surface foil}} = \vartheta_{\text{wall}} - \frac{\dot{Q}_{\text{el}} \cdot d}{\lambda \cdot A} \quad [^\circ\text{C}] \quad (2)$$

The heat  $\dot{Q}_{\text{el}}$  of the electrically heatable aluminium block is measured to be 180 W. With the thickness of the foil  $d = 0,2 \text{ mm}$ , the thermal conductivity of stainless steel  $\lambda = 15 \text{ W/mK}$  and the effective heat transfer area  $A = 0,4 \text{ cm}^2$  a temperature on the surface of the metallic foil  $T_{\text{surface foil}}$  of 39°C is calculated. The effective heat transfer area  $A$  is calculated by

$$A = n \cdot w \cdot l_{\text{channel}} \quad [\text{cm}^2] \quad (3)$$

Due to the turbulent flow conditions ( $\text{Re} > 2300$ ) the Nusselt number is calculated to  $\text{Nu} = 23$ . The heat transfer coefficient  $\alpha$  of the device for the aqueous solution is calculated via the Nusselt number by

$$\alpha = \frac{\text{Nu} \cdot \lambda_{\text{fluid}}}{d_h} \quad [\text{W/m}^2\text{K}] \quad (4)$$

to  $\alpha = 77630 \text{ W/m}^2\text{K}$  ( $\lambda_{\text{fluid}} = 0,612 \text{ W/mK}$ ,  $d_h = 178 \mu\text{m}$ ). The temperature measured in the aqueous solution is nearly as high as the temperature of the metallic foil estimated by (2). This can be related to the high heat transfer coefficient of about 77630  $\text{W/m}^2\text{K}$ . The low temperature of the metallic foil indicates that the heat transfer resistance is located in the heat transfer through the metallic foil. It can easily be seen that the choice of a different surface material with a

higher thermal conductivity like aluminium or copper should result in an increase of the temperature of the surface of the metallic foil. Hence due to the high  $\alpha$ -value an increase of the temperature of the aqueous solution should be the consequence. Thus the higher temperature of the metallic foil (made of aluminium or copper, coated or non-coated) in the microstructured device should cause an additional layer by the precipitation of calcium carbonate.

## RESULTS

Figure 5a-c shows the mass flow in dependence on time for the different surface materials. In all cases the mass flow is kept nearly constant to a level of about 1,5 kg/h. The mass flow in the specific experiments differs about 5% depending on the settings of the pump used for the experiments.

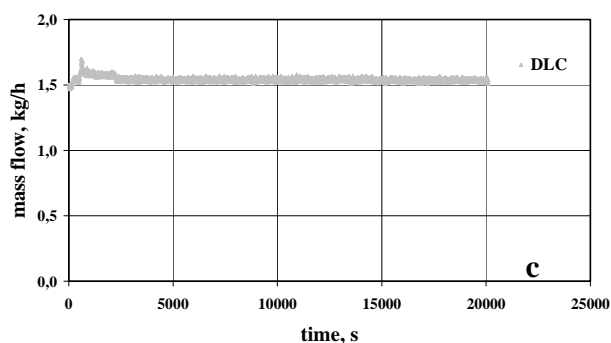
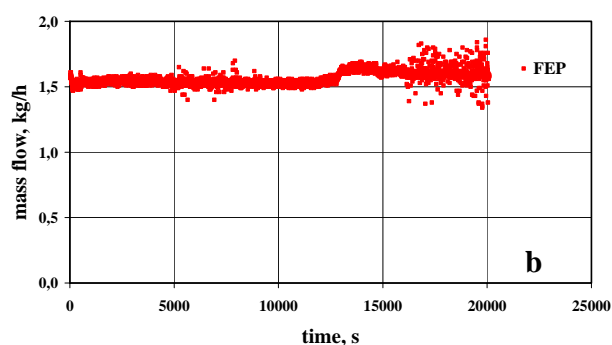
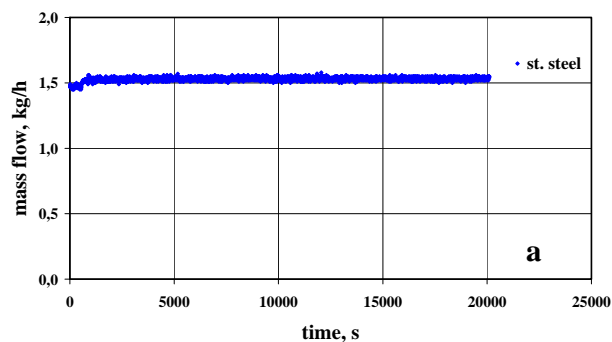


Figure 5 a-c: mass flow in dependence on time for different surface materials (stainless steel, FEP, DLC).

Figure 6 shows the pressure drop  $\Delta p$  in dependence on time for the different surface materials. In all three cases we find a parallel run of the curves at the beginning of the experiments. After the incubation time of 5400 seconds (90 minutes) a small increase of the slope can be observed. At 12000 seconds (200 minutes) the curves split up and continue with different slopes. The experiment done with the uncoated stainless steel foil results in the highest pressure drop of about 0,38 bar after 20000 seconds (330 minutes). The DLC coated foil results in a pressure drop of about 0,3 bar and the FEP coated foil yields in the lowest pressure drop of about 0,14 bar after 20000 seconds (330 minutes). It has to be taken into account that the pressure transducers used have a working range of about 10 bars.

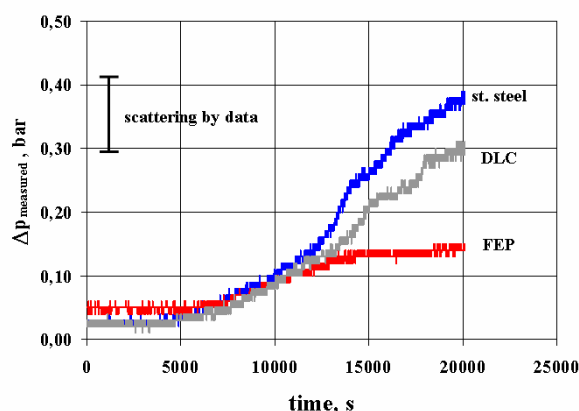


Figure 6: pressure drop  $\Delta p$  in dependence on time for different surface materials (stainless steel, FEP, DLC)

In Figure 7-9 photos of the disassembled main item of the micro heat exchanger are shown. In the upper picture the microstructured device and in the lower picture the foil is shown. In every case the inlet is on the left side, the outlet is on the right side respectively. The microstructured device and the foil are covered by a layer of calcium carbonate mainly in the area of the channels and in the outlet area. The formation and precipitation of calcium carbonate starts immediately when the solution enters the channels. The main part of the particles can be realized in the right channel section where the highest temperature is reached. White particles can also be found in the half-moon shaped outlet area. The particles will be transported away by the mass flow running through the channels and cumulate in this area.

But it attracts attention that in the disassembled micro heat exchanger most of the white particles stick to the channel walls of the microstructured device and not to the heat transfer surface itself. This observation can be explained by two considerations.

- Calcium carbonate precipitates on the heat transfer surface and the crystals grow up into the cross section of the channel geometry.
- The low flow velocity of 0,3 m/s in the laminar flow regime ( $Re=110$ ) and the thermal conductivity of water of 0,652 W/mK result in a temperature equalisation across the flow direction. At this elevated temperature the formation and precipitation of calcium carbonate takes also place in the bulk of the fluid.

In both cases the particles can stick to the wall of the channels and cause an increase of the pressure drop. A few particles will be transported out of the channels and deposited in the outlet area.

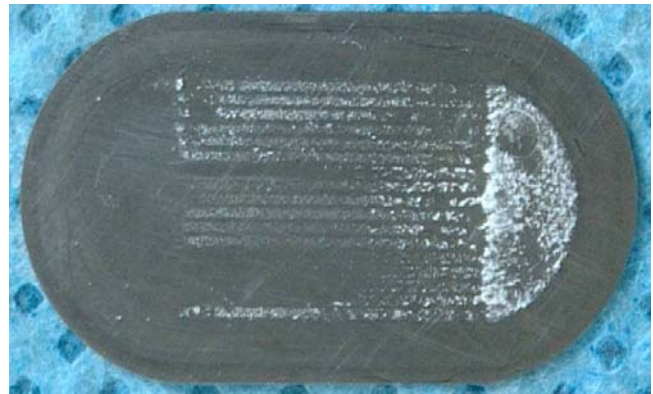
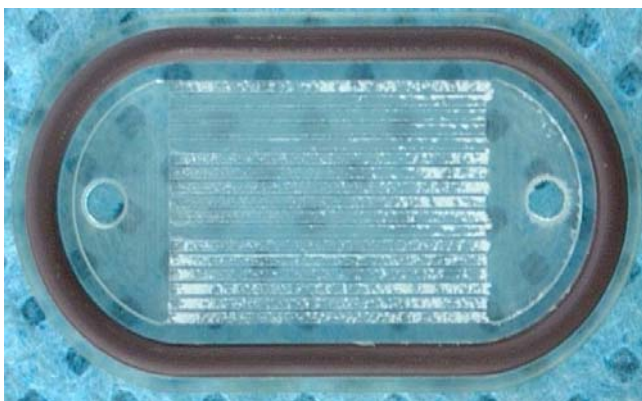


Figure 7: microstructured device and metallic foil (stainless steel) of the disassembled microstructured heat exchanger.

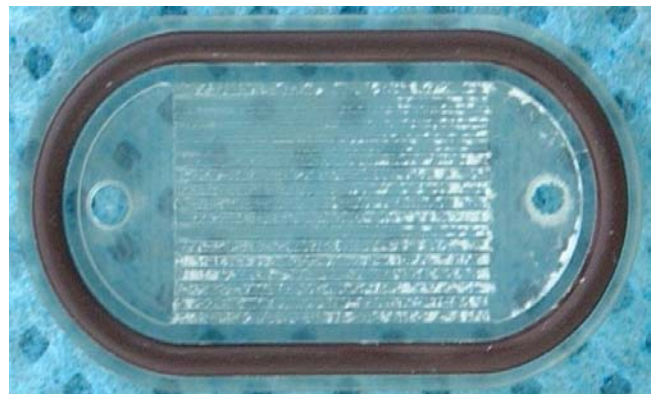


Figure 8: microstructured device and metallic foil (DLC) of the disassembled microstructured heat exchanger.

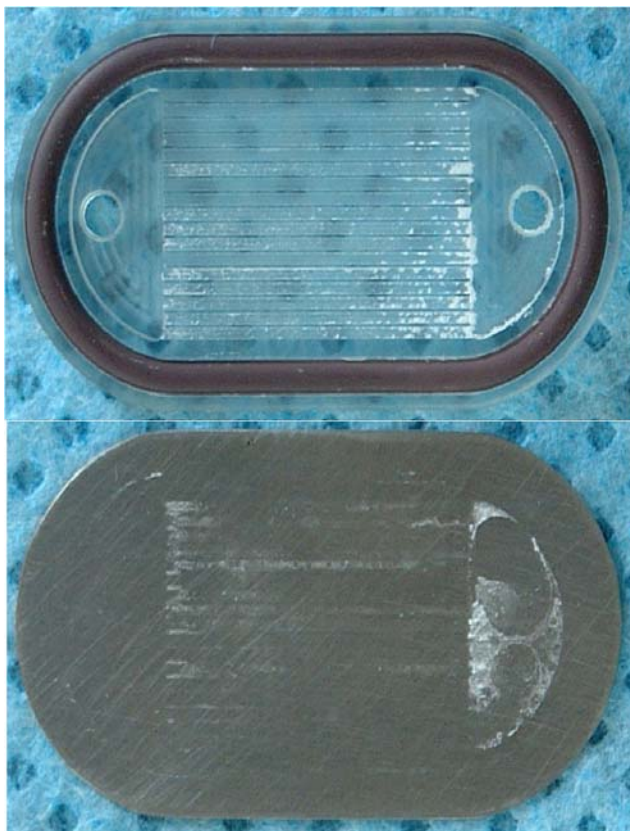


Figure 9: microstructured device and metallic foil (FEP) of the disassembled microstructured heat exchanger.

The temperature of the outgoing aqueous solution continuously decreases and hence the heat flux  $\dot{Q}$ . The FEP coated foil has a lower thermal conductivity than stainless steel, which results in lower temperature of the outgoing solution at the beginning of the experiment. The experiment with DLC coated foil starts with a higher heat flux. This can be related to the pump settings, which shows a higher flow rate in the beginning. After the incubation time of 90 minutes a decrease of the slopes of all curves can be observed. After 330 minutes all curves reach approximately the same value.

Figure 10a-c shows the fouling resistance in dependence on time for the different surface materials. The figure shows the influence of the coatings on induction period and on the gradient of the fouling plot. For all materials the same fouling tendency is found. After the incubation time of 90 minutes the real fouling period starts. In the incubation time itself single crystals on the heat transfer surface may influence the flow resulting in an increased turbulence. This leads to an increased heat transfer and, hence, to negative values of the fouling resistance. In the fouling period an increase of the slopes

can be observed. This gradient is the same for all three curves. All curves end in the same value of the fouling resistance after a test run of 330 minutes. Each curve shows the well known asymptotic behaviour.

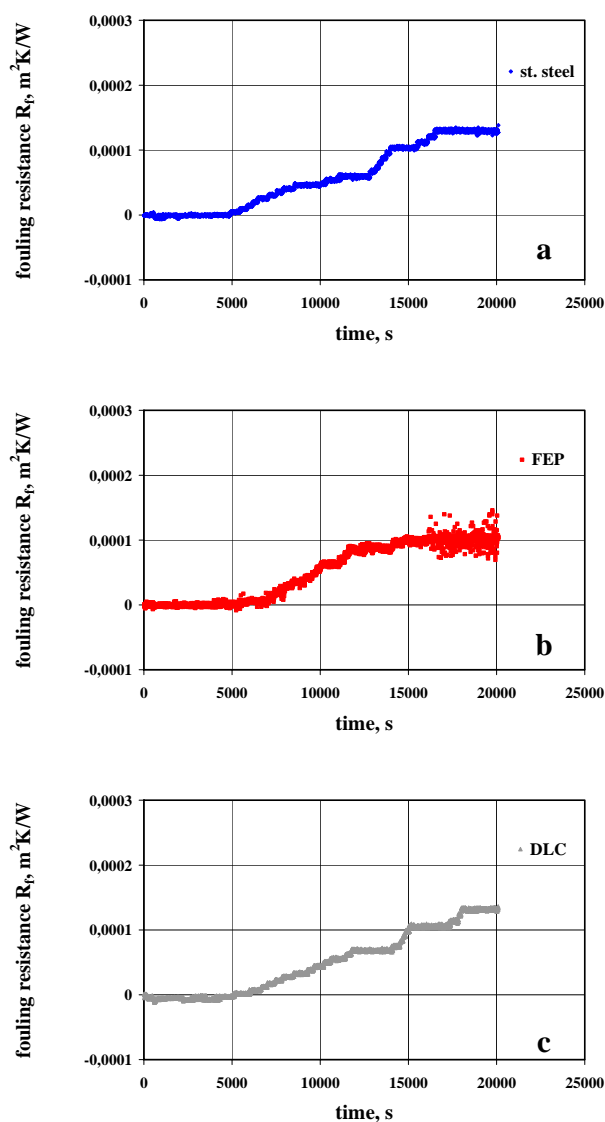


Figure 10a-c: fouling resistance  $R_f$  in dependence on time for different surface materials (stainless steel, FEP, DLC)

## DISCUSSION

The results for all materials, the uncoated stainless steel and the DLC and FEP coated heat transfer surfaces, show typical fouling behaviour with an induction period, followed by an asymptotic built-up of the deposited calcium carbonate. The fouling plot of DLC and FEP coated heat

transfer surfaces contradict the hypothesis that the use of such materials leads to much longer induction periods. There is no influence to see of the surface material on the induction period and the gradient of the fouling period.

It is described in the literature that heat transfer surfaces modified with coatings having outstanding interfacial characteristics result in a mitigation of fouling (Förster et al., 1999, 1999, and 2000; Augustin et al. 1995). Depending on the characteristics of the coating an improvement of the induction period as well as the fouling period is found. This strategy mainly influences the duration of the induction period. Fouling consists of two processes, a deposition process and a removal process, respectively. The removal process depends on two factors: the shear stress forces due to the fluid flow and the adhesive strength of the substances to the surface.

The experiments described in the literature are based on different heat exchanger systems excluding microstructured heat exchanger. All the systems have in common that they have large geometrical dimensions in comparison to a microstructured heat exchanger. In microchannels dominate laminar flow conditions due to the small channel dimensions, which are in the regime of a few  $\mu\text{m}$ . In a heat exchanger system like a plate heat exchanger turbulent flow conditions are obtained. Deposits caused by fouling exceeding the laminar boundary layer are exposed to the shear stress forces of the turbulent flow. The deposit is removed by the flow.

Coatings with outstanding interfacial characteristics and turbulent flow conditions may influence the fouling by increasing the duration of the induction period. For this reason first orientating tests in the turbulent flow regime have been performed in a micro heat exchanger. But the heat transfer resistance is located in the metallic foil itself made of the stainless steel. Stainless steel with its low thermal conductivity does not result in a surface temperature high enough to cause precipitation of calcium carbonate. Thus higher temperatures of the metallic foil in the microstructured device should only be reached with metallic foils made of e.g. copper or aluminium.

## CONCLUSIONS

Micro heat exchangers may substantially prone to fouling due to their narrow channels geometries as well as their high heat transfer coefficients. In this study a closer look to the influence of different surface materials on the fouling in the laminar flow regime was taken. It was found that there seems to be no influence of the surface material on the induction period and on the gradient of the fouling period. The fouling behaviour of all three materials is similar.

First orientating tests in the turbulent flow regime have also been performed. But the use of a material with low thermal conductivity (metallic foil made of stainless steel) which transfers the heat from the heat source to the aqueous solution demonstrates the high performance of the microstructured heat exchanger. On the other hand due to this high performance the temperature for the build-up of the additional layer couldn't be reached.

Further investigations especially in the turbulent flow regime will proceed. The influence of different anti-fouling layers seems to be a promising research topic.

## NOMENCLATURES

### Latin symbols

|                       |  |                               |
|-----------------------|--|-------------------------------|
| $A$                   | effective heat transfer area                     | $\text{m}^2$                  |
| $d$                   | thickness of the foil                            | $\text{mm}$                   |
| $d_h$                 | hydraulic diameter                               | $\mu\text{m}$                 |
| $k_0$                 | overall heat transfer coeff. (clean surface)     | $\text{m}^2\text{K}/\text{W}$ |
| $k_f$                 | overall heat transfer coeff. (encrusted surface) | $\text{m}^2\text{K}/\text{W}$ |
| $n$                   | number of channels                               | -                             |
| $T$                   | temperature                                      | $^\circ\text{C}$              |
| $\text{Nu}$           | Nusselt number                                   | -                             |
| $\dot{Q}$             | heat flux  | $\text{W}$                    |
| $\dot{Q}_{\text{el}}$ | heat (electrical)                                | $\text{W}$                    |
| $\text{Re}$           | Reynolds number                                  | -                             |
| $R_f$                 | fouling resistance                               | $\text{W}/\text{m}^2\text{K}$ |
| $\Delta p$            | pressure drop                                    | $\text{bar}$                  |
| $w$                   | width of the channels                            | $\mu\text{m}$                 |
| $l$                   | length of the channels                           | $\mu\text{m}$                 |
| FEP                   | fluorinated ethylene propylene                   | -                             |
| DLC                   | diamond like carbon                              | -                             |

### Greek symbols

|                           |  |                               |
|---------------------------|--|-------------------------------|
| $\alpha$                  | heat transfer coefficient                                      | $\text{W}/\text{m}^2\text{K}$ |
| $\lambda$                 | thermal conductivity   | $\text{W}/\text{mK}$          |
| $\vartheta_{\text{wall}}$ | temperature of the metallic block underneath the metallic foil | $^\circ\text{C}$              |

### Subscripts

|              |                 |
|--------------|-----------------|
| inlet        | inlet position  |
| outlet       | outlet position |
| fluid        | fluid           |
| channel      | channel         |
| surface foil | surface foil    |



**REFERENCES**

Augustin, W., Bohnet, M., Influence of the Ratio of Free Hydrogen Ions on Crystallization Fouling, *Chem. Eng. Process.* 34 (1995), S. 79-85.

Förster, M., Augustin, W., Bohnet, M., Influence of the adhesion force crystal/heat exchanger surface on fouling mitigation, *Chem. Eng. and Proc.* 38 (1999) 4-6, S. 449-461.

Förster, M., Bohnet, M., Influence of the Interfacial Free Energy Crystal/Heat Transfer Surface on the Induction period during Fouling, *Int. J. Th. Sci.* (1999) 38, S. 944-954.

Förster M., Bohnet M., Modification of Molecular Interactions at the Interface Crystal/Heat Transfer Surface to Minimize Heat Exchanger Fouling, *International Journal of Thermal Sciences* (2000) 39, S. 697-708.

Lund, D., Sandu, C., "State-Of-The-Art of Fouling: Heat Transfer Surfaces", S. 27-56 in Hallström, Bengt, Fundamentals and applications of surface phenomena associated with fouling and cleaning in food processing: Proceedings from an internat. workshop arranged by Div. of Food Engineering, Lund Univ., Alnarp, Sweden, Tyloesand, Sweden, April 6 - 9, 1981.

Schubert, K., Bier, W., Brandner, J.J., Fichtner, M., Franz, C., Linder, G., Realization and Testing of Microstructure Reactors, "Micro Heat Exchangers and Micromixers for Industrial Applications in Chemical Engineering", Proceedings, 2<sup>nd</sup> International Conference on Microreaction Technology, New Orleans, USA, march 8-12, 1998

Schubert, K. Brandner, J.J., Fichtner, M., Linder, G., Schygulla, U., Wenka, A., Microstructured Devices for Applications in Thermal and Chemical Process Engineering, *Microscale Thermophysical Engineering*, Vol. 5 No. 1, 2001, pp. 17-39.

Wörz, O., Jäckel, K., Richter, Th., Wolf, A., "Microreactors, a New Efficient Tool for Optimum Reactor Design", Proceedings, 2<sup>nd</sup> International Conference on Microreaction Technology, New Orleans, USA, march 8-12, 1998

Shah, R.K., London, A.L., Laminar Flow Forced Convection in Ducts, Academic Press, New York 1978

Tautz, H., 1971, *Wärmeleitung und Temperaturausgleich*, Verlag Chemie, Weinheim, Germany